

Virtual Sensing of Photovoltaic Module Operating Parameters

Lappalainen, Kari; Manganiello, Patrizio; Piliouline, Michel; Spagnuolo, Giovanni; Valkealahti, Seppo

DOI

[10.1109/JPHOTOV.2020.2972688](https://doi.org/10.1109/JPHOTOV.2020.2972688)

Publication date

2020

Document Version

Final published version

Published in

IEEE Journal of Photovoltaics

Citation (APA)

Lappalainen, K., Manganiello, P., Piliouline, M., Spagnuolo, G., & Valkealahti, S. (2020). Virtual Sensing of Photovoltaic Module Operating Parameters. *IEEE Journal of Photovoltaics*, 10(3), 852-862. Article 9018387. <https://doi.org/10.1109/JPHOTOV.2020.2972688>

Important note

To cite this publication, please use the final published version (if applicable). Please check the document version above.




Copyright

Other than for strictly personal use, it is not permitted to download, forward or distribute the text or part of it, without the consent of the author(s) and/or copyright holder(s), unless the work is under an open content license such as Creative Commons.

Takedown policy

Please contact us and provide details if you believe this document breaches copyrights. We will remove access to the work immediately and investigate your claim.

Virtual Sensing of Photovoltaic Module Operating Parameters

Kari Lappalainen , Member, IEEE, Patrizio Manganiello , Member, IEEE, Michel Piliouguine, Giovanni Spagnuolo , Fellow, IEEE, and Seppo Valkealahti, Member, IEEE

Abstract—The single diode equivalent circuit allows describing photovoltaic panels behavior quite accurately. The values of the five parameters appearing in this model are usually identified in standard test conditions, at which irradiance and temperature values are given. Instead, when this identification has to be performed on field, suitable environmental sensors are required. In this article, a procedure for the on-site identification of the single diode model parameters as well as of the working irradiance and temperature conditions is presented. The procedure operates only on the measured panel current versus voltage curve, or on a part of it around the maximum power point, and does not need any other input data. A consolidated identification algorithm, effectively running on any embedded system for on-site application, is used. The proposed procedure is validated through a large number of experimental measurements acquired in two different geographic locations.

Index Terms—Condition monitoring, diagnosis, parameters identification, photovoltaic (PV) systems.

I. INTRODUCTION

PHOTOVOLTAIC (PV) panels are frequently modeled through the single diode model (SDM) shown in Fig. 1 [1]. It is a good tradeoff between complexity and accuracy including a current generator, the dc current thereof mainly depending on the irradiance at which the panel works, a diode, which models the PN junction, and two resistors reproducing the power loss mechanisms.

The parameters appearing in this model are the photoinduced current I_{ph} , the saturation current I_s , and the ideality factor η of the diode and the shunt and the series resistances R_{sh} and R_s , respectively. By this model, the PV current I is calculated for every positive value of the PV voltage V , by solving a nonlinear

Manuscript received December 21, 2019; revised January 22, 2020; accepted February 3, 2020. Date of publication February 28, 2020; date of current version April 21, 2020. The work of Patrizio Manganiello was supported by the European Union's Horizon 2020 research and innovation programme under the Marie Skłodowska-Curie under Grant 751159. The work of Giovanni Spagnuolo was supported by Tampere University, Finland. (Corresponding author: Giovanni Spagnuolo.)

Kari Lappalainen and Seppo Valkealahti are with Tampere University, 3370 Tampere, Finland (e-mail: kari.lappalainen@tuni.fi; seppo.valkealahti@tuni.fi).

Patrizio Manganiello is with the IMEC (partner in EnergyVille), 3600 Genk, Belgium, and also with the Delft University of Technology, 2628 Delft, The Netherlands (e-mail: p.manganiello@tudelft.nl).

Giovanni Spagnuolo is with the University of Salerno, 84084 Salerno, Italy (e-mail: gspagnuolo@unisa.it).

Michel Piliouguine is with the University of Salerno, 84084 Salerno, Italy (e-mail: mpiliouginerocha@unisa.it).

Color versions of one or more of the figures in this article are available online at <http://ieeexplore.ieee.org>.

Digital Object Identifier 10.1109/JPHOTOV.2020.2972688

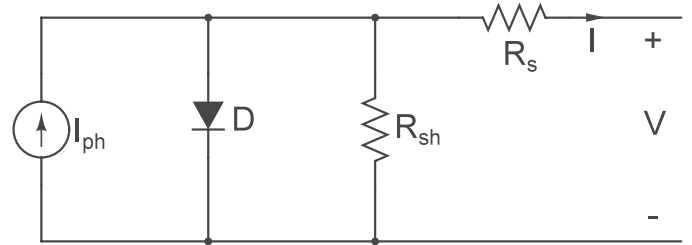


Fig. 1. Circuit diagram of the single diode model.

equation or by using the following explicit expression, which employs the Lambert W -function [1]

$$I = \frac{R_{sh}(I_{ph} + I_s) - V}{R_s + R_{sh}} - \frac{a}{R_s} W(\theta) \quad (1)$$

with

$$\theta = \frac{R_s R_{sh} I_s}{a(R_s + R_{sh})} e^{\frac{R_s R_{sh}(I_{ph} + I_s) + R_{sh} V}{a(R_s + R_{sh})}} \quad (2)$$

and

$$a = \frac{N_s \eta k T}{q} \quad (3)$$

In (3), N_s is the number of series-connected cells in the panel, k is the Boltzmann constant and q is the electron charge. In addition to the explicit dependency on the cell temperature T , in Kelvin, shown in (3), the photo induced and saturation currents show major dependencies on the irradiance level G , and on the cell temperature T that have to be taken into account. Indeed, the photoinduced current exhibits the following dependency law [2]:

$$I_{ph} = \frac{G}{G_{STC}} [I_{ph,STC} + \alpha_I (T - T_{STC})] \quad (4)$$

where α_I is the thermal coefficient of the panel short-circuit current and all the quantities having the subscript STC are referred to the standard test conditions, that are $G_{STC} = 1 \text{ kW/m}^2$ and $T_{STC} = 298.15 \text{ K}$. Values of parameters in STC are typically given by the manufacturer in the panel data sheet. The cell temperature also significantly affects the PV cell saturation current, according to the following equation:

$$I_s = C_{STC} T^3 e^{-\frac{q E_g(T)}{k T}} \quad (5)$$

where C_{STC} is a coefficient that is calculated at STC [1] and $E_g(T)$ is the material band gap, in eV, at the temperature T ,

which is determined as follows [3]:

$$E_g(T) = E_{g,STC} [1 + \alpha_E \cdot (T - T_{STC})] \quad (6)$$

wherein, for crystalline silicon cells, the energy bandgap in STC is $E_{g,STC} = 1.121$ eV and the thermal coefficient of the energy gap is assumed to be equal to $\alpha_E = -0.000277$ K⁻¹. The analytical model given by (1)–(6) is commonly used for simulating the PV module at any couple $\{G, T\}$, provided that the values of the five parameters

$$P_{STC} = \{I_{ph,STC}, I_{s,STC}, \eta_{STC}, R_{s,STC}, R_{sh,STC}\} \quad (7)$$

have been identified in STC. This goal can be achieved in different ways and the current literature proposes many possible approaches. Some of them use optimization algorithms for minimizing the root mean square error (RMSE) between the STC current versus voltage (I – V) curve provided by the manufacturer and the curve obtained by the identified set of parameters [4]. An effective application of the optimization algorithms often requires the careful analysis of the search space [5]. Other approaches, e.g., [6], [7], symbolically manipulate a set of five nonlinear equations in order to reduce it to a smaller one that is, again, solved by a minimization algorithm. Moreover, some papers propose the use of an approximated set of five equations allowing to calculate the five parameters explicitly, thus without using iterative numerical procedures [1].

Unfortunately, only few papers are dedicated to the identification of the five parameters $\{I_{ph}, I_s, \eta, R_s, R_{sh}\}$ in operating conditions that are neither the STC one nor any other at given $\{G, T\}$ values. Some methods, which are almost the same used in STC, require to measure the actual $\{G, T\}$ values through suitable irradiance and temperature sensors. The latter ones measure the ambient temperature or the temperature at the panel backside [8]; literature formulae for predicting the cell temperature T from those measurements are also used [7], [9]. For instance, in [7] some translation formulae are used for identifying the values of the five parameters at the given $\{G, T\}$ condition. A simple and straightforward approach, which is based on explicit formulas, is presented in [10]. It uses a novel relation between the diode ideality factor and the open-circuit voltage and it has as its input the actual $\{G, T\}$ couple.

Some studies in literature, instead of being focused on the identification of all the five parameters, address the identification of the series resistance R_s value only. Indeed, it is the most significant one for the assessment of the PV module state of health. In [11], a recent and comprehensive overview can be found. In [12], the shunt resistance is neglected and some experimental current–voltage couples allow to evaluate the series resistance as a function of the slope of the I – V curve close to the open-circuit conditions. Measurements noise and the voltage range in which the experimental points are linearly fitted may affect this estimation significantly [13]. The approach presented in [14] defines some diagnostic indicators, with the increase of the series resistance that is detected through the variation of the slope of the I – V curve in the vicinity of the maximum power point. In [15], the so-called “Suns-Voc analysis” is used for analyzing the outdoor behavior of the modules. An improvement of the method has been more recently introduced in [16]: therein

the real-time series resistance is monitored without the need of measuring the whole I – V curve. These methods require the measurement of the operating irradiance and temperature values of the module and also some data collected in a time window preceding the instant at which the identification is performed. The method proposed in [17] does not require the whole I – V curve and it is based on a relationship expressing the value of the open-circuit voltage as a function of the series resistance and of the current and voltage values in the maximum power point. Unfortunately, a precharacterization of the module is required: it is used to identify the values of three coefficients, which are strictly dependent on the type of module under test, appearing in the defined interpolating function. In [18] the effects of the variation of η , R_s and R_{sh} values on the I – V curve are analyzed. It results that the same change of the I – V curve might be due to the variation of even more than one parameter, this making the identification of the parameter that is responsible for that change quite complicated. The proposed identification method is oriented to the detection of production defects and can be applied offline, since tests at a low and fixed irradiance level are required, which is not feasible in outdoor conditions. A set of I – V curves measured at different irradiance levels but with a constant cell temperature is also required by the approach presented in [19].

The numerical approach proposed in this article does not identify the five SDM parameters of a PV panel. Instead, by exploiting the well-known dependency that some of them have on the operating irradiance and temperature, the proposed algorithm is aimed at identifying the working conditions, thus $\{G, T\}$, and the values of a reduced set of the SDM parameters of the PV panel during its outdoor operation.

The main objective of the procedure presented in this article is the computation of the series resistance R_s and of the shunt resistance R_{sh} without measuring G and T . As a byproduct, the approach provides an estimation of the actual G and T values by means of the electrical model of the photovoltaic device. There are some methods in the literature to identify those variables by using the short-circuit current I_{SC} and the open-circuit voltage V_{OC} , respectively. Unfortunately, they require the PV panel operating point moves away from the maximum power point (MPP), with a consequent power loss. In the final part of this article, instead, it is shown that the main advantage offered by the approach presented in this article is that it allows to have a good estimation of the two resistances and of G and T by sampling the I – V curve only in a small interval close to the MPP, even during the normal operation of the PV panel, thus avoiding energy losses.

The method uses the full identified set of parameters $\{I_{ph,STC}, I_{s,STC}, \eta_{STC}, R_{s,STC}, R_{sh,STC}\}$ in STC determined through explicit formulas as guess solution of a numerical procedure exploiting (1)–(6) to identify some parameters in real operating conditions. Because of its low computational burden, it has a high potential of being implemented in a low cost embedded processor for on-site applications, e.g., incorporated into a micro inverter or a power optimizer. Identification of the actual values of parameters such as R_s and R_{sh} provides information about the current state of health of the PV panel.

Thus, the proposed approach can be further extended to develop PV module monitoring and diagnostic algorithms.

The rest of this article is organized as follows. Section II describes the numerical approach. Section III shows how the algorithm performs in different conditions by using a huge number of experimental data. Section IV is dedicated to conclusions and possible applications of the algorithm.

II. IDENTIFICATION ALGORITHM

The algorithm assumes that the type and model of the PV panel, as well as the technology used for the PV cells it is made of, are given. Thus, the values of the parameters $\{\alpha_I, \alpha_E, E_{g,STC}\}$ referred to STC, appearing in (4) and (6), respectively, are known. Their values are fixed at their respective STC values regardless of the operating conditions of the panel. This allows determining the values of the five SDM parameters $\{I_{ph,STC}, I_s,STC, \eta,STC, R_s,STC, R_{sh,STC}\}$ in STC by using one of the methods presented in the literature. Because the proposed procedure should be designed for an on-site application and running on an embedded system, the more suitable procedures for the computation of the SDM parameters in STC are those ones using explicit formulas or quickly converging iterative procedures. The method presented in [1] appears to be a good candidate. It has been shown in the literature that this approach guarantees accurate parameters identification in STC with a low computational effort. A feasible option should be also the method in [20], which is widely recalled in the literature.

The achieved set of parameters in STC (7) is used as a guess solution for the following numeric procedure. The $I-V$ curve of the PV panel working in outdoor conditions is assumed to be the input to the proposed algorithm. No additional information about the PV panel operating conditions, especially the G and T values, is assumed to be given as input to the proposed procedure. According to (3)–(6), G and T have a nonlinear effect on the model (1) that is used for the identification.

According to the literature [3], the diode ideality factor has been kept fixed at its STC value $\eta = \eta_{STC}$. Thus, the identification problem has been scaled down to four parameters $\{I_{ph}, I_s, R_s, R_{sh}\}$. Moreover, it has been noted that formulas (4)–(6) give the relationship between $\{I_{ph}, I_s\}$ and $\{G, T\}$, so that the four parameters to identify can be turned into

$$P = \{G, T, R_s, R_{sh}\}. \quad (8)$$

Thus, a fitting procedure is set up to identify the values of these four parameters: it is based on the minimization the RMSE between the $I-V$ curve given by the SDM (1) and the experimental one. The identification process has been performed by using a classical Trust Region nonlinear minimization approach, with a termination condition fixed on both the RMSE value and the identified parameter values. Both termination tolerances have been fixed at 10^{-10} . Guess solution to start the minimization method is based on (7), thus it is $\{G_{STC}, T_{STC}, R_{s,STC}, R_{sh,STC}\}$.

Fig. 2 shows the flowchart of the proposed procedure for a single $I-V$ curve. It can be applied as well to a sequence of $I-V$ curves acquired time by time on the same PV panel. In the latter

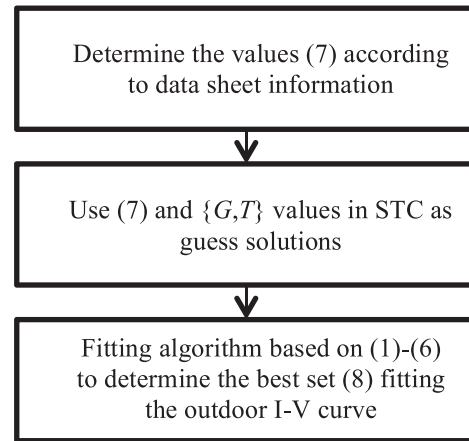


Fig. 2. Flowchart of the proposed procedure.

TABLE I
ELECTRICAL PARAMETERS OF THE NAPS PANEL
AND OF THE ISOFOTON PANEL IN STC

Parameter	NAPS panel	Isofoton panel
I_{sc} [A]	8.00	6.54
I_{MPP} [A]	7.36	5.88
V_{oc} [V]	33.0	19.8
V_{MPP} [V]	25.8	16.00
α_I [A/K]	0.0047	0.0027
α_V [V/K]	-0.124	-0.071

case, especially if the time interval between two consecutive acquisitions is not too large, the guess solution for the fitting algorithm can be the algorithm output set (8) achieved for the previous $I-V$ curve. Such a loop has been used for obtaining the results shown in the following section.

III. EXPERIMENTAL RESULTS

The experimental data used in this article refer to PV panels available at Tampere University [21] and at the University of Malaga [22]. The former ones are Naps Solar Systems Ltd. (NAPS) NP190GKg PV panels, which include 54 polycrystalline silicon cells. The latter ones are Isofoton panels I-94/12 type including 2 parallel connected strings of 33 cells each. Their electrical performance in STC, as it is reported in the datasheet, is summarized in Table I.

As a first step, the five parameters of the single diode model in STC have been identified through the explicit formulas proposed in [1]. The achieved sets of parameters are shown in Table II.

It is worth noting that if the well-known procedure [20] is used, the values achieved for the sets of parameters in Table II are quite close to those ones listed therein. Thus, the results presented in the following of this article remain the same.

Some of these parameter values have been used to define the search space and to provide the guess solution of parameters for the Trust Region minimization algorithm used for the identification. Tables III and IV collect these values, which refer to the irradiance and temperature and to the series and shunt

TABLE II
SDM PARAMETERS FOR THE NAPS PANEL AND
FOR THE ISOFOTON PANEL IN STC

Parameter	NAPS panel	Isofoton panel
$I_{ph,STC}$ [A]	8.00	6.54
$I_{s,STC}$ [nA]	1.6993	0.9852
η_{STC}	1.0686	1.0326
$R_{s,STC}$ [Ω]	0.3786	0.1879
$R_{sh,STC}$ [Ω]	122.56	47.64

TABLE III
GUESS SOLUTION AND SEARCH SPACE OF THE FOUR
PARAMETERS TO IDENTIFY FOR THE NAPS PANEL

Parameter	Guess solution	Range
G [W/m^2]	1000	[10,1300]
T [$^{\circ}C$]	25	[0,70]
R_s [Ω]	0.3786	[0.1,5]
R_{sh} [Ω]	122.56	[50,500]

TABLE IV
GUESS SOLUTION AND SEARCH SPACE OF THE FOUR PARAMETERS TO
IDENTIFY FOR THE ISOFOTON PANEL

Parameter	Guess solution	Range
G [W/m^2]	1000	[10,1300]
T [$^{\circ}C$]	25	[0,120]
R_s [Ω]	0.1879	[0,100]
R_{sh} [Ω]	47.64	[1,50000]

resistances. It is worth noting that the guess solution is based on data referring to STC conditions taken from Table II and the ranges are determined quite easily on the basis of the typical working conditions of the cells, thus G and T in the installation site, and of typical values of the two resistances appearing in the SDM.

A. First Example

The first identification test has been done by processing four hours of operation of the NAPS PV panel. One I - V curve per second is measured. Thus, the parameters $\{G, T, R_s, R_{sh}\}$ have been identified, in sequence, for the 14 400 I - V curves of the set. Each curve has been acquired by sampling the voltage range $[0, V_{oc}]$ in 4000 points.

For the first curve, the guess solution has been the one shown in Tables III. Because each curve has been acquired 1 s after the previous one, from the second curve on the guess solution has been settled as the identified set of parameters $\{G, T, R_s, R_{sh}\}$ of the previous curve. It is worth noting that the validation of the method has not been done on one single curve, because only a partial validation of the performance of the method would have been achieved. An analysis on a long sequence of curves and different operating conditions is useful also for having an idea of the potential use of the proposed approach in real PV control, monitoring and diagnostic applications.

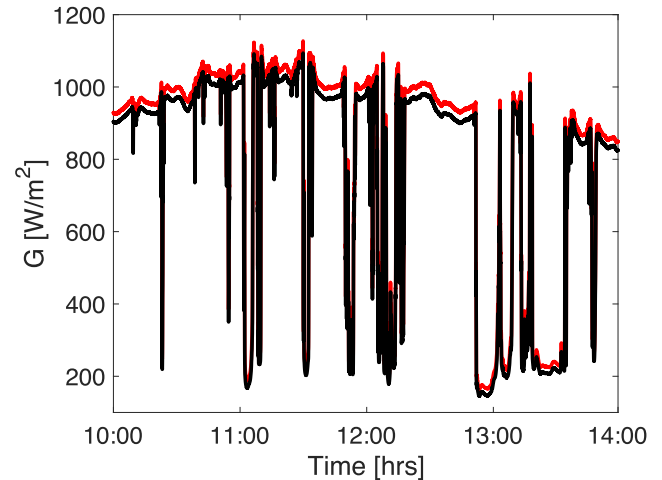


Fig. 3. Measured (black) and identified (red) irradiances in the first example.

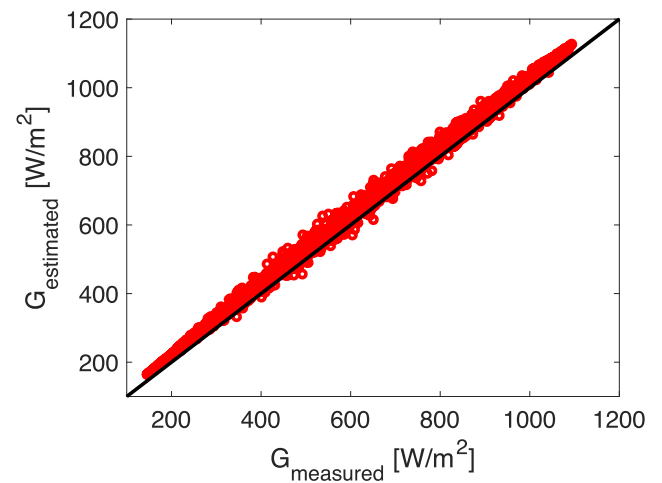


Fig. 4. Scatter plot of the estimated (y-axis) versus measured (x-axis) irradiances in the first example.

Fig. 3 shows the comparison between the irradiance level G identified by the procedure and the one measured by a pyranometer [21]. The overestimation of the measured irradiance has been assessed to be due to a value of the short-circuit current in STC declared by the PV panel manufacturer that is smaller than the real one. As it comes out from (4), and since the method [1] for the identification of the set of parameters in STC assumes that $I_{ph,STC} = I_{sc,STC}$, an $I_{sc,STC}$ value that is smaller to the one that is really corresponding to G_{STC} leads to an overestimation of the identified value of G . Some experimental tests done on the panel by measuring the ratio I_{sc}/G in different conditions reveal that measured short-circuit current is higher than the one declared by the manufacturer in the data sheet in STC. Comparison of the experimental measurement and the identified values in Fig. 4 confirms the slight overestimation.

Figs. 5 and 6 show the comparison between the measured and the estimated temperatures. It is worth remarking that the measured values are acquired through a PT100 sensor placed on the backside surface of the PV panel [21]. Instead, the estimated

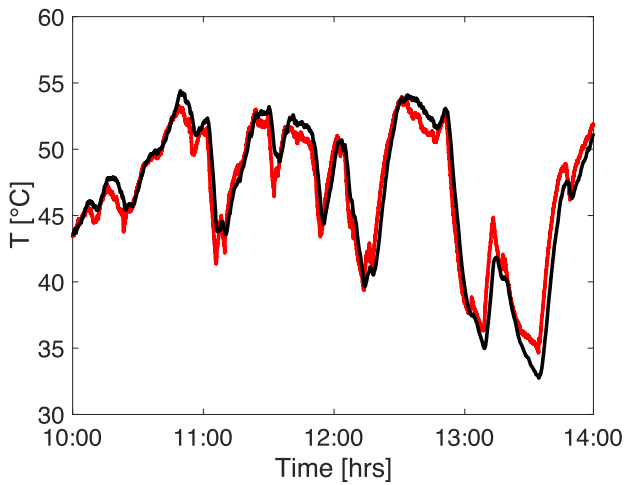


Fig. 5. Measured panel backside (black) and identified cell (red) temperatures in the first example.

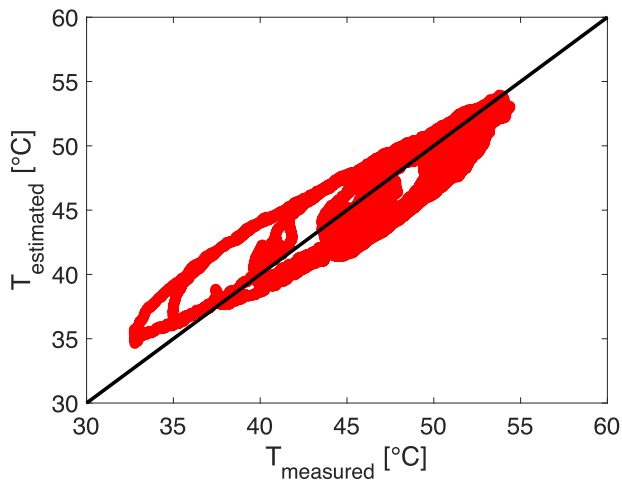


Fig. 6. Scatter plot of the estimated cell temperature (y-axis) versus measured panel backside temperature (x-axis) in the first example.

temperature is the cell's one, as it is evident from (3)–(6) used in the model. The temperature difference between the PV cell and the backside of the PV panel increases linearly with the increase of the irradiance received by the panel. Thus, the cell temperature can be estimated to be several Celsius degrees higher than the panel backside temperature at 1 kW/m^2 irradiance by using the PV panel material heat conductivities documented in literature [23]. Consequently, the identification of the cell temperature achieved through the proposed approach is reasonably accurate. The accuracy, of both G and T , has to be considered in relation with the simple model used as virtual sensor.

As stated in the previous section, for each I – V curve, also the values of series and shunt resistances have been identified. The results for the full sequence of 14 400 I – V curves are shown in Figs. 7 and 8 for R_s and R_{sh} , respectively. R_{sh} keeps always at high values, in some cases, reaching the upper bound fixed in Tables III. The minimization method used for the parametric identification explores the upper part of the R_{sh} range

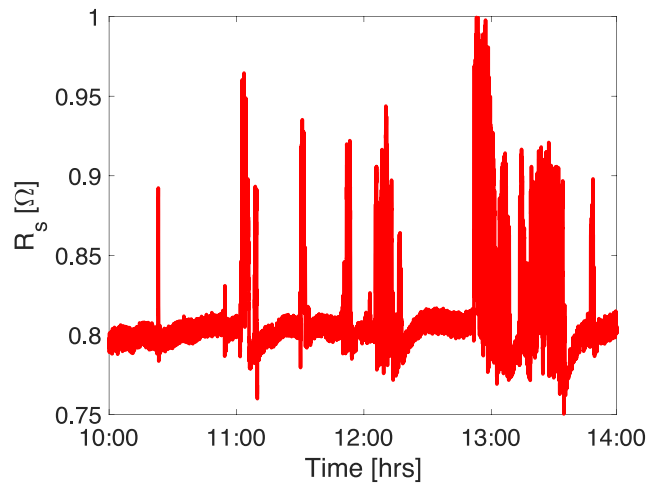


Fig. 7. Identified series resistance values in the first example.

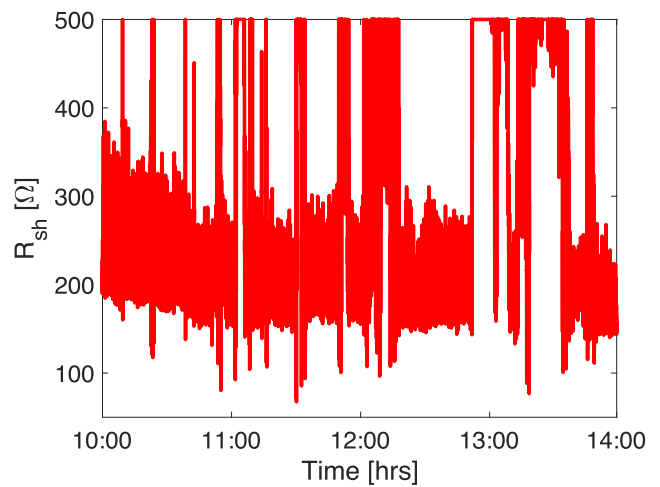


Fig. 8. Identified shunt resistance values in the first example.

without improving the accuracy significantly. This happens especially at low irradiance levels, where R_s reaches a higher value. Both these behaviors are also documented in [2] and [24]. The identified value of the series resistance at high irradiance can be compared with the STC one in Table II considering that the measurements on the PV panel are not performed exactly at the panel's terminals. Indeed, two cables of 53.5 m length and having a total equivalent resistance of $0.363 \text{ } \Omega$ are used for acquiring the I – V curves in the Tampere University laboratory.

B. Second Example

A second set of I – V curves for the NAPS panel acquired during the operation in Tampere has been considered. It again refers to four hours of PV panel operation in real conditions. Low irradiance and low-temperature conditions have been considered in this case, in order to highlight the limit of the proposed approach in such conditions. Figs. 9 and 10 show the measured and identified G and T . As for the first example, the temperature is measured at the backside of the PV panel; instead, the cells

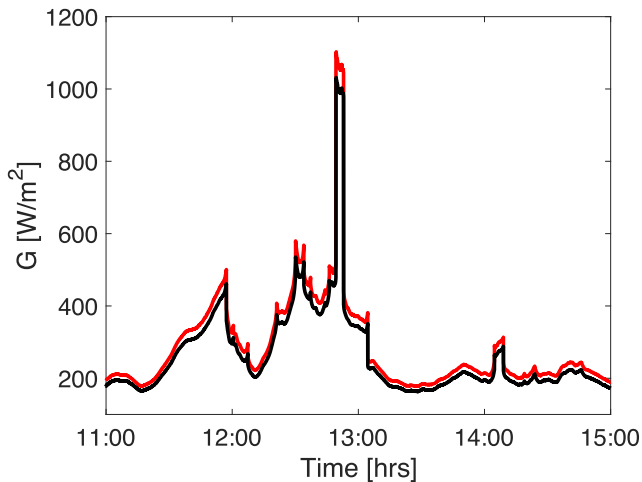


Fig. 9. Identified (red) and measured (black) irradiance values in the second example.

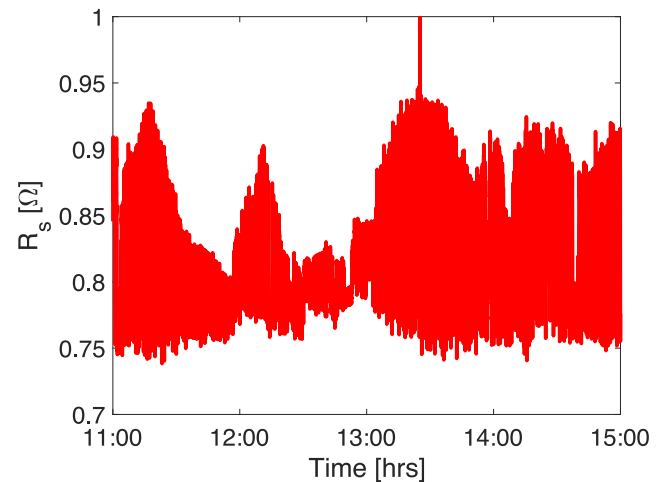


Fig. 11. Identified series resistance in the second example.

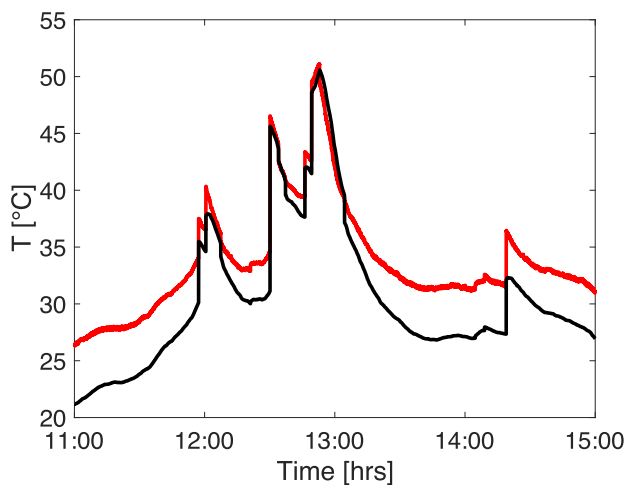


Fig. 10. Identified (red) cell and measured (black) panel backside temperatures in the second example.

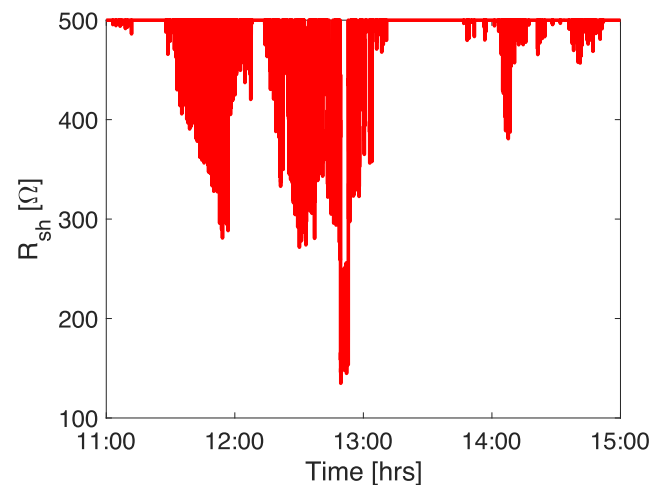


Fig. 12. Identified shunt resistance in the second example.

temperature has been identified through the method presented in this article. Figs. 9 and 10 put into evidence that, although the model catches the variations and the overall behavior, the estimation error increases clearly with decreasing irradiance. The reason of this is in the well-known limitations of the SDM and of the equations adopted when the operating conditions move far from the STC. These limitations of the used model are visible, in particular, in the identified PV cell temperature in Fig. 10 when irradiance fluctuates between high and very low values. The estimated series and shunt resistances are shown in Figs. 11 and 12, respectively. Their magnitudes are in line with those ones obtained in the previous test case, but their variation is much larger. Since this second example considers mainly low irradiance conditions, the identified shunt resistance keeps almost always very high, often reaching the upper bound of the search space. This behavior is consistent with the results shown in the previous section and also with the literature, where the shunt resistance has been claimed to be proportional to the inverse of the irradiance level.

C. Third Example

A further test has been done starting from the same set of NAPS panel I - V curves used in the first example. In addition, for each curve, only a reduced number of samples around the MPP have been considered. Indeed, in real applications, the PV panel energy production might be too much penalized by the scan of the whole I - V curve, also at low current and voltage values, hence close to V_{oc} and I_{sc} . Thus, only the points in the range $[V_{MPP} - 3 \text{ V}, V_{MPP} + 3 \text{ V}]$ have been considered for each I - V curve. This range corresponds to almost one-fifth of the range $[0, V_{oc}]$ and the power production is not too much penalized as the PV panel is working around its MPP during normal operation, e.g., driven by a Perturb and Observe MPP Tracking method.

In Fig. 13, an example of I - V curve identification is shown. The black points around the MPP are the only ones used for the parametric identification based on the algorithm proposed in this article. As expected, the identification of the constant-current part of the curve, including I_{sc} , is less accurate than the

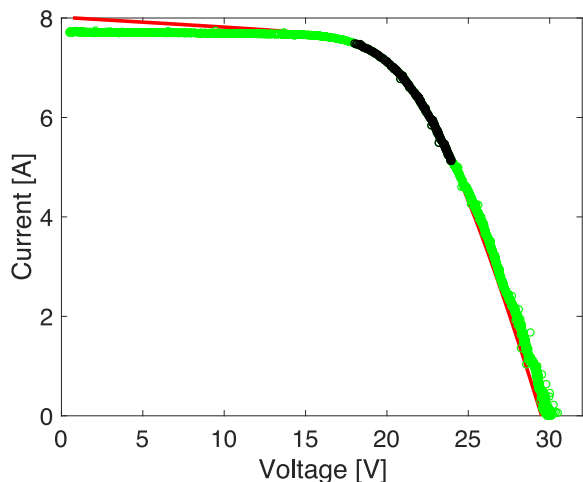


Fig. 13. Example of measured I - V samples (green), samples used for the identification (black) and the fitted I - V curve (red) of the PV panel.

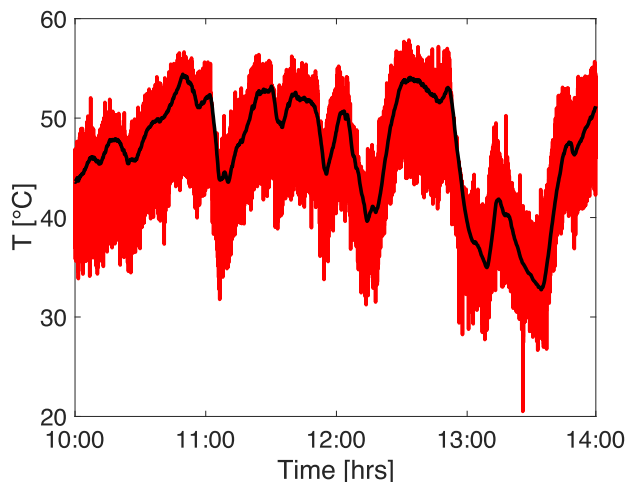


Fig. 15. Measured (black) PV panel backside and identified (red) cell temperatures in the third example.

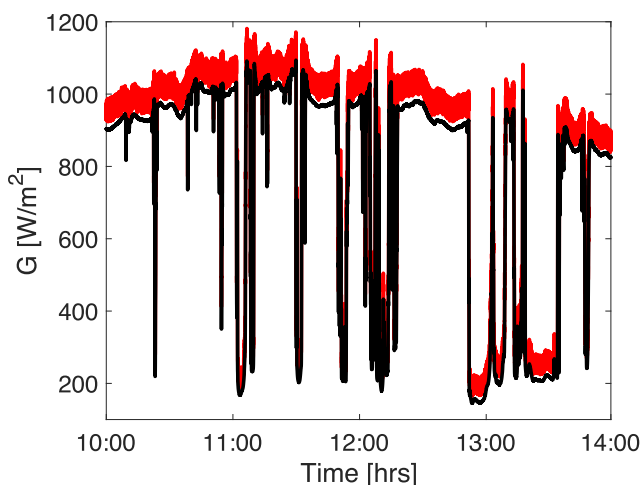


Fig. 14. Measured (black) and identified (red) irradiance values in the third example.

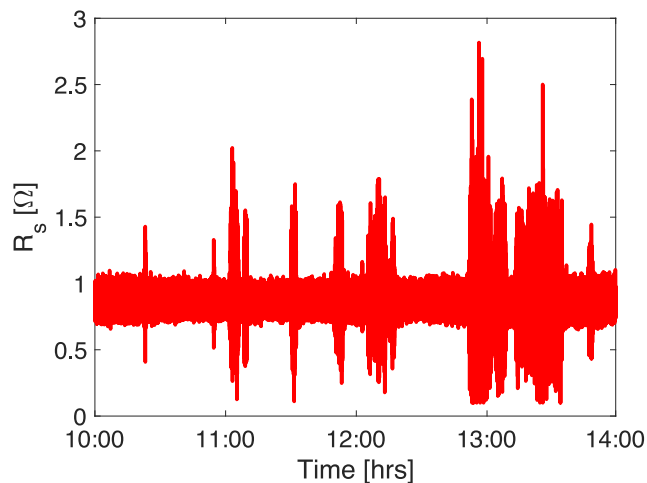


Fig. 16. Identified values of the series resistance in the third example.

constant-voltage one, including V_{oc} . This is evident by looking at the red curve, which is the one reconstructed by using the parameters identified by means of the black samples only. The choice of a symmetric interval around the voltage value where the MPP occurs is the main reason of such inaccuracy. The higher slope of the curve at the right side of the MPP covers a larger portion of the curve thereof, leading to a better curve fitting at high voltages.

By comparing the red curve of the identified irradiance in Fig. 14 with the corresponding one in Fig. 3, it is evident that the intelligibility of the reconstructed G is not seriously compromised. The curve is at first hand just more noisy because of the less accurate identification of the short-circuit current, as it has been demonstrated in Fig. 13. The identified temperature is also affected by identification noise accordingly, as can be noticed by comparing Fig. 15 with Fig. 5. The R_s identification is an apparent sequel of these results, as it can be seen in Fig. 16. The two R_s identifications are compared in Fig. 17. In black color, the series resistance identified using all the samples of

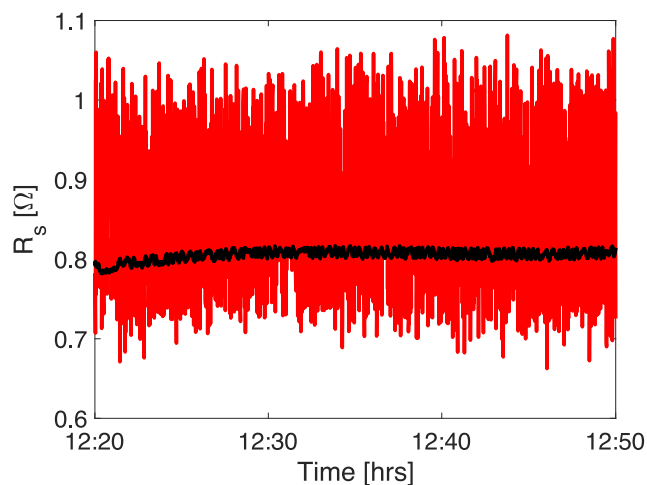


Fig. 17. Identified series resistances in the case of identification through the whole I - V curve (black) and through the samples in the range $V_{MPP} \pm 3$ V (red).

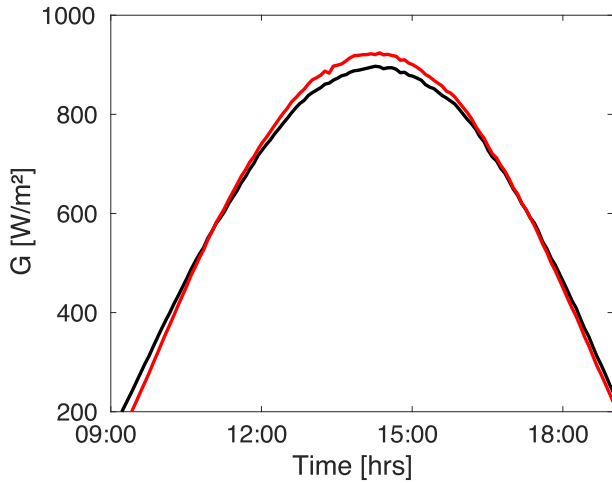


Fig. 18. Measured (black) and identified (red) irradiances for the test concerning the Isofoton PV panel.

the curve as in the first example discussed in Section III-A (see Fig. 7) is shown. In red color, the series resistance identified as proposed in this section is depicted. The comparison has been limited to a time interval corresponding to high irradiance level. The noisy curve based on the reduced samples gives a slight overestimation, on the average, with respect to the more accurate parameter identification based on the full I - V curve. As expected, the reduced number of samples used for the identification reduces the accuracy and increases the variation of identified R_s values recognized through the proposed method.

Instead of considering the samples of the I - V curve in a fixed range of voltages around the MPP, it should be more reasonable to take the samples in a power range defined as a percentage of the power delivered by the panel at the MPP: the smaller the range, the higher the MPPT efficiency. For this example, the experimental data referring to the Isofoton panel operating in Malaga have been considered. In this case, one I - V curve consisting of 130 samples is acquired every 3 min. Figs. 18 and 19 show the G and T values measured by a Kipp&Zonen CMP21 pyranometer and a four wires RTD Pt100 sensor placed at the back side of the panel, respectively [22].

It is worth noting the accurate identification result achieved in this case, because of a clear sky measurement and especially because of data sheet values that are more realistic for the Isofoton panel with respect to the ones referred to the NAPS panel used. The good agreement in terms of cells temperature has been also achieved, thanks to the correction formula proposed in [8] relating the measured T_m and the cell T temperatures through a coefficient ΔT related to the type of lamination of the module, glass/cell/polymer for the Isofoton panel and the installation configuration (open rack in this case)

$$T = T_m + \frac{G}{G_{STC}} \cdot \Delta T. \quad (9)$$

In the sequel, the value $\Delta T = 3$ °C has been used. Fig. 20 shows a comparison among different methods used for the estimation of the panel series resistance. The reference value

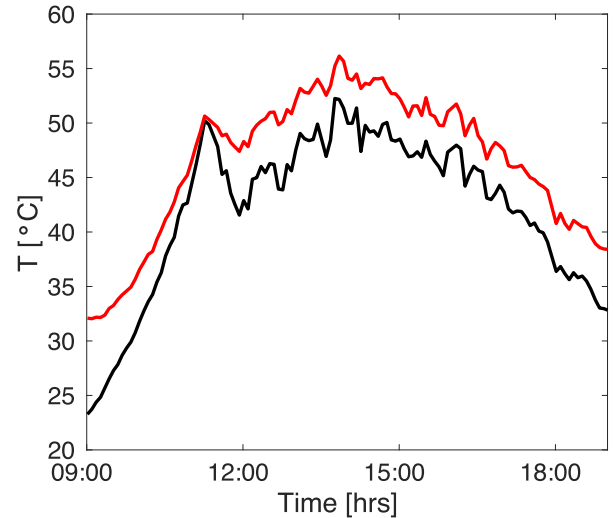


Fig. 19. Measured (black) and identified (red) cell temperatures for the test concerning the Isofoton PV panel.

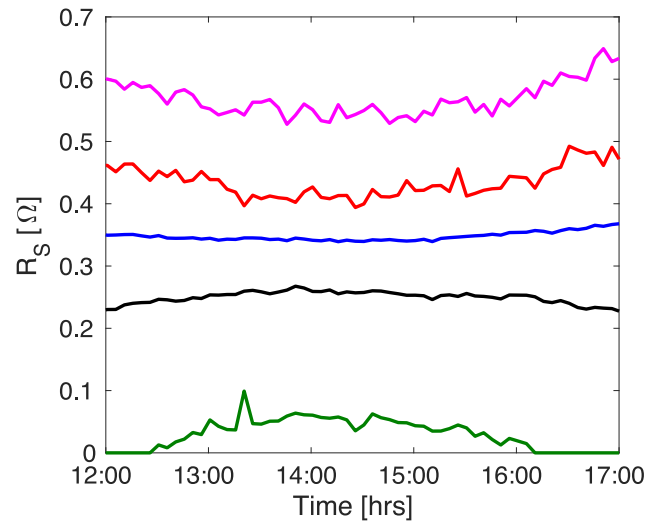


Fig. 20. Identification of the R_s through some methods: green curve = method [25], black curve = reference value, blue curve = proposed method, red curve = proposed method using points ensuring at least the 90% of the power delivered at the MPP, magenta curve = method [16].

(black curve) is obtained by numerical fitting of the experimental I - V curve by using the SDM (1) and having as input also the measured T values. The proposed method gives an evident overestimation of the series resistance, especially if a limited number of samples around the MPP are used. Fig. 21 shows what are the samples considered for applying the fitting procedure used in this article and giving the R_s values corresponding to the red curve in Fig. 20. The acquisition of these samples ensures that the panel produces a power level that is not lower than 90% of the power in the MPP. In Fig. 21, in black color, the 39 points on a total of 130 samples that ensure a power that is at least the 90% of the one in the MPP are evidenced.

It is worth noting that other methods, e.g., [16] and [25], give a larger overestimation or a significant underestimation of

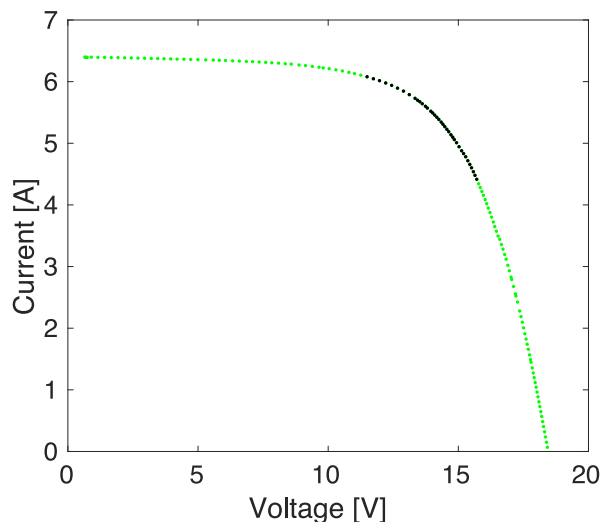


Fig. 21. One of the I - V curves related to the Isofoton panel. The black samples are the operating points at which the panel delivers at least the 90% of the power at the MPP.

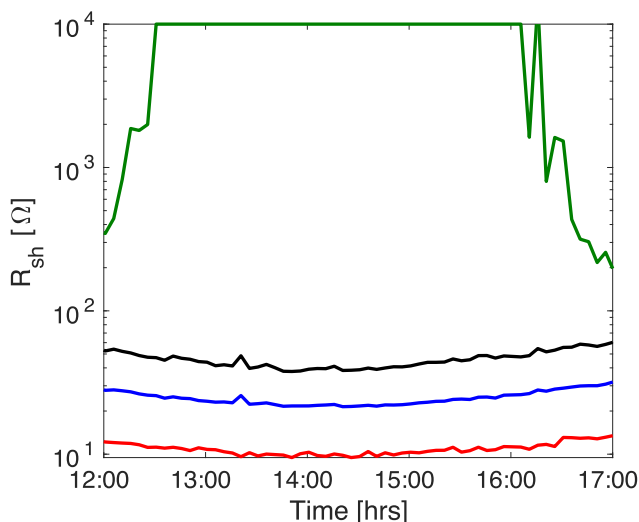


Fig. 22. Identification of the R_{sh} through some methods: green curve = method [25], black curve = reference value, blue curve = proposed method, red curve = proposed method using points ensuring at least the 90% of the power delivered at the MPP.

the panel series resistance. The former approach suffers from the additional drawback of requiring a training set of information based on measurements acquired under low irradiance conditions.

The latter method [25] suffers from the fact that it uses a SDM scaled down to four parameters, e.g., neglecting the R_s at the two extremes of the time window considered in Figs. 18 and 19. The same comparison done in Fig. 20 is performed through Fig. 22 by referring to the shunt resistance values. It is worth noting that the method [16] does not address the identification of R_{sh} and that the method [25] in the central part of the day scales the number of SDM parameters down by setting the shunt resistance at an infinite value. The identification procedure followed in this

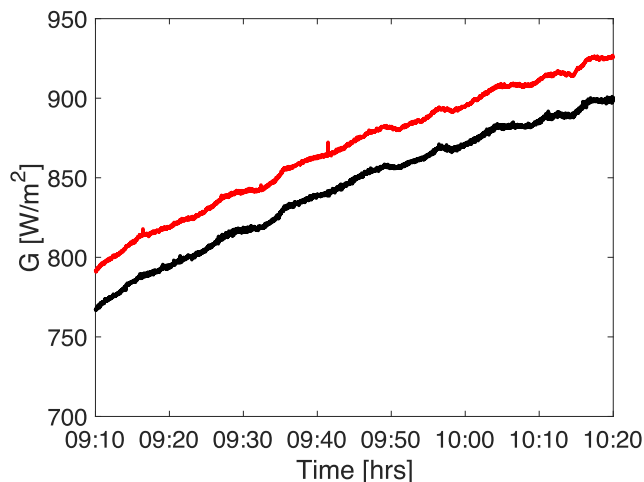


Fig. 23. Identified (red) and measured (black) irradiance for the string of 17 panels in the fourth example.

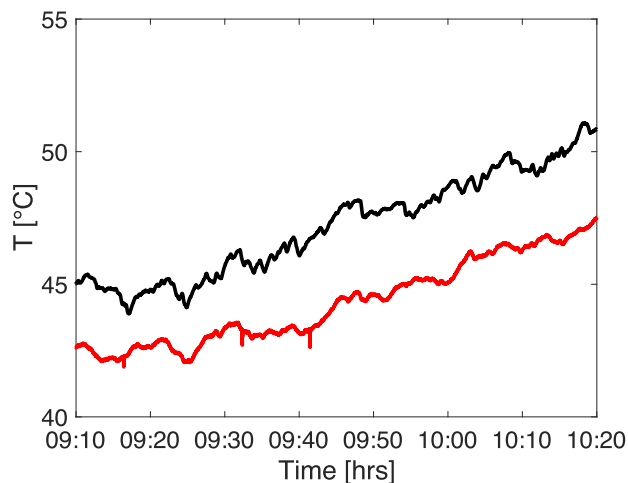


Fig. 24. Identified (red) cell temperature and measured (black) temperature at the backside of one of the 17 panels in the string in the fourth example.

article ensures a good identification of the shunt resistance value even for diagnostic purposes.

D. Fourth Example

The last example refers to a series connected string of 17 NAPS PV panels of the same type used in the previous examples and tested in Tampere. The irradiance sensor is attached to the same panel where the temperature sensor is installed. In this example, the panels may not operate under uniform G and T conditions, which may cause larger differences between identified and measured values. Figs. 23 and 24 show also in this case a reasonable accuracy of the identified irradiance and temperature, respectively. One must again take into account the inaccuracy of the data sheets values and the difference between the PV panel backside temperature and the cells temperature. The latter discrepancy is also accentuated by the uneven distribution of the temperature among the cells of the 17 panels in series. The series resistance identification shown in Fig. 25 indicates an average

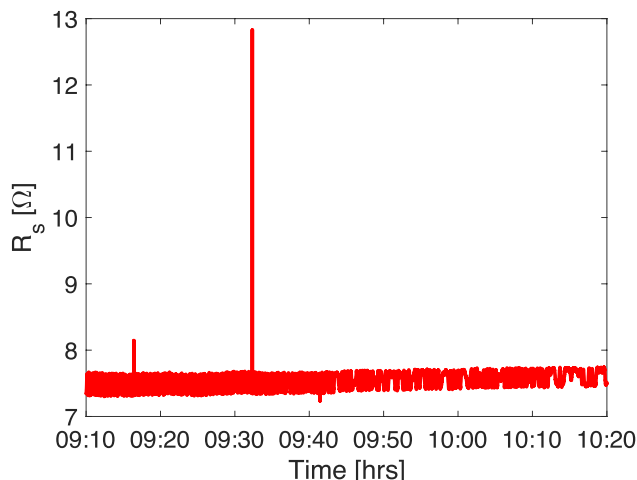


Fig. 25. Identified series resistance of the string of 17 panels in the fourth example.

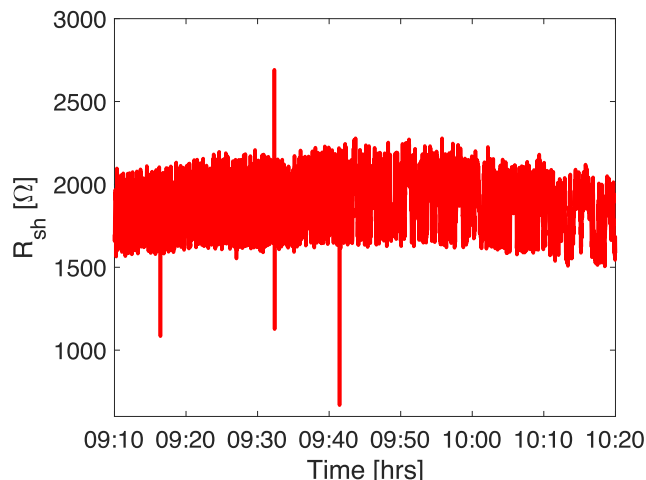


Fig. 27. Identified shunt resistance of the string of 17 panels in the fourth example.

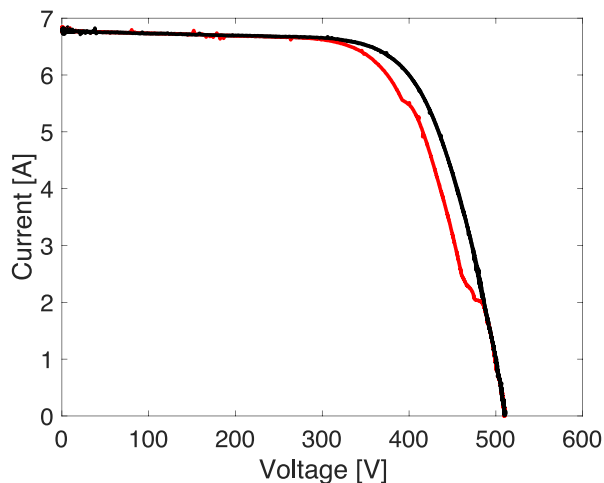


Fig. 26. Measured I - V curve corresponding to the inaccurate parameter identification in the case of partial shading conditions (red), and I - V curves measured one second before and one second after under uniform conditions (black, superimposed).

value that is compatible with the one obtained for the single panel at high irradiance (see Fig. 7). It is worth noting that some anomalous identified R_s values are due to a temporary mismatch affecting the string. This is clearly shown in Fig. 26 where three I - V curves are plotted: in black color, the two I - V curves acquired one second before and one second after the event corresponding to the highest observed R_s value (just after 9:30). In red color instead, the mismatched curve acquired in that instant and giving rise to the incorrect identification. This is evidently due to the fact that the considered model is not able to operate on I - V curves corresponding to mismatched conditions. The identified shunt resistance values are shown in Fig. 27. The effect of anomalous identification is also evident in few cases.

IV. CONCLUSION

In this article, an algorithm for the identification of the operating parameters of a PV generator is presented. The approach takes as input only the I - V curve acquired in the actual operating conditions and the STC measurements that are commonly made available by the manufacturer through the PV panel data sheet. The approach is based on well-assessed relationships giving the dependency of some parameters appearing in the single diode model from the irradiance and temperature. The algorithm has been tested on several cases by using outdoor experimental measurements taken in two different locations on two types of panels. The accuracy and limitations of the virtual sensor for G , T , R_s , and R_{sh} , especially at low irradiance levels, have been documented and they were not unexpected. The identification of the two resistances appears to be more accurate than the one given by other methods in the literature, even if a small number of samples are acquired around the MPP. This is compatible with MPPT operation and minimizes the power losses due to the acquisition of the samples of the I - V curve close to short-circuit and open-circuit conditions. Further work is in progress for investigating the advantages of including more involved dependencies of the SDM parameters on G and T in the used model. Given the relationship between the estimated parameters and the state of health of the PV panels, the proposed approach can be further extended for developing monitoring and diagnostic algorithms, also in consideration of its possible implementation on an embedded system for on-field operation even as a tool integrated into panel-dedicated electronics.

ACKNOWLEDGMENT

The work of Giovanni Spagnuolo was supported by Tampere University, Finland. IMEC is a partner in EnergyVille (www.energyville.be), a collaboration between the Flemish research partners KU Leuven, VITO, imec, and UHasselt in the field of sustainable energy and intelligent energy systems. The authors acknowledge University of Malaga (SPAIN) for having made available some experimental data sets used in this paper.

REFERENCES

- [1] G. Petrone, C.A. Ramos Paja, and G. Spagnuolo, *Photovoltaic Sources Modeling*. Hoboken, NJ, USA: Wiley, 2017.
- [2] C.W. Hansen, "Parameter estimation for single diode models of photovoltaic modules," Sandia Nat. Lab., Albuquerque, NM, USA, SAND2015-2065, 2015.
- [3] W. De Soto, S. Klein, and W. Beckman, "Improvement and validation of a model for photovoltaic array performance," *Sol. Energy*, vol. 80, no. 1, pp. 78–88, 2006.
- [4] A. R. Burgers, J. A. Eikelboom, A. Schonecker, and W. C. Sinke, "Improved treatment of the strongly varying slope in fitting solar cell I–V curves," in *Proc. Conf. Rec. 25th IEEE Photovolt. Spec. Conf.*, 1996, pp. 569–572.
- [5] A. A. Cárdenas, M. Carrasco, F. Mancilla-David, A. Street, and R. Cárdenas, "Experimental parameter extraction in the single-diode photovoltaic model via a reduced-space search," *IEEE Trans. Ind. Electron.*, vol. 64, no. 2, pp. 1468–1476, Feb. 2017.
- [6] E. Moshksar and T. Ghanbari, "Adaptive estimation approach for parameter identification of photovoltaic modules," *IEEE J. Photovolt.*, vol. 7, no. 2, pp. 614–623, Mar. 2017.
- [7] M. Hejri and H. Mokhtari, "On the comprehensive parametrization of the photovoltaic (PV) cells and modules," *IEEE J. Photovolt.*, vol. 7, no. 1, pp. 250–258, Jan. 2017.
- [8] D. L. King, W. E. Boyson, and J. A. Kratochvill, "Photovoltaic array performance model," Sandia Nat. Lab., Albuquerque, NM, USA, ARep. SAND2004-3535, 2004.
- [9] G. Ciulla, V. Lo Brano, and E. Moreci, "Forecasting the cell temperature of PV modules with an adaptive system," *Int. J. Photoenergy*, vol. 2013, 2013 Art. no. 192854.
- [10] E. I. Batzelis and S. A. Papathanassiou, "A method for the analytical extraction of the single-diode PV model parameters," *IEEE Trans. Sustain. Energy*, vol. 7, no. 2, pp. 504–512, Apr. 2016.
- [11] R. Singh, M. Sharma, R. Rawat, and C. Banerjee, "An assessment of series resistance estimation techniques for different silicon based SPV modules," *Renew. Sustain. Energy Rev.*, vol. 98, pp. 199–216, Dec. 2018.
- [12] D. Sera, R. Teodorescu, and P. Rodriguez, "Photovoltaic module diagnostics by series resistance monitoring and temperature and rated power estimation," in *Proc. 34th Annu. Conf. IEEE Ind. Electron.*, 2008, pp. 2195–2199.
- [13] A. J. Bühler, F. Perin Gasparin, and A. Krenzinger, "Post-processing data of measured I–V curves of photovoltaic devices," *Renew. Energy*, vol. 68, pp. 602–610, 2014.
- [14] S. Spataru, D. Sera, T. Kerekes, and R. Teodorescu, "Diagnostic method for photovoltaic systems based on light I–V measurements," *Sol. Energy*, vol. 119, pp. 29–44, Sep. 2015.
- [15] M. K. Forsyth, M. Mahaffey, A. L. Blum, W. A. Dobson, and R. A. Sinton, "Use of the suns-Voc for diagnosing outdoor arrays & modules," in *Proc. IEEE Photovolt. Spec. Conf.*, 2014, pp. 1928–1931.
- [16] M. G. Deceglie, T. J. Silverman, B. Marion, and S. R. Kurtz, "Real-Time series resistance monitoring in PV systems without the need for I–V curves," *IEEE J. Photovolt.*, vol. 5, no. 6, pp. 1706–1709, Nov. 2015.
- [17] J. S. Stein, S. McCaslin, C. W. Hansen, W. E. Boyson, and C. D. Robinson, "Measuring PV system series resistance without full IV curves," in *Proc. IEEE 40th Photovolt. Spec. Conf.*, 2014, pp. 2032–2036.
- [18] S. Bowden and A. Rohatgi, "Rapid and accurate determination of series resistance and fill factor losses in industrial silicon solar cells," in *Proc. Eur. Photovolt. Sol. Energy Conf.*, 2001, pp. 1–10.
- [19] C. W. Hansen and B. H. King, "Determining series resistance for equivalent circuit models of a PV module," *IEEE J. Photovolt.*, vol. 9, no. 2, pp. 538–543, Mar. 2019.
- [20] M. G. Villalva, J. R. Gazoli, and E. R. Filho, "Comprehensive approach to modeling and simulation of photovoltaic arrays," *IEEE Trans. Power Electron.*, vol. 24, no. 5, pp. 1198–1208, May 2009.
- [21] D. Torres Lobera, A. Mäki, J. Huusari, K. Lappalainen, T. Suntio, and S. Valkealahti, "Operation of TUT solar PV power station research plant under partial shading caused by snow and buildings," *Int. J. Photoenergy*, vol. 2013, 2013, Art. no. 837310.
- [22] M. Piliouguine, J. Carretero, L. Mora-López, and M. Sidrach-de-Cardona, "Experimental system for current–voltage curve measurement of photovoltaic modules under outdoor conditions," *Prog. Photovolt., Res. Appl.*, vol. 19, no. 5, pp. 591–602, 2011.
- [23] A. S. Armstrong and W.G. Hurley, "A thermal model for photovoltaic panels under varying atmospheric conditions," *Appl. Thermal Eng.*, vol. 30, pp. 1488–1495, 2010.
- [24] A. Mermoud and T. Lejeune, "Performance assessment of a simulation model for PV modules of any available technology," in *Proc. 25th Eur. Photovolt. Sol. Energy Conf.*, 2010, pp. 4786–4791.
- [25] S. Cannizzaro, M. C. Di Piazza, M. Luna, and G. Vitale, "PVID: An interactive Matlab application for parameter identification of complete and simplified single-diode PV models," in *Proc. IEEE 15th Workshop Control Model. Power Electron.*, 2014, pp. 1–7.